IJCRT.ORG ISSN : 2320-2882

INTERNATIONAL JOURNAL OF CREATIVE RESEARCH THOUGHTS (IJCRT)

An International Open Access, Peer-reviewed, Refereed Journal

Performance Analysis of Graphene-Based Fractal Dipole Antennas and Split Ring Resonators: A Comparative Study with Copper

[1] Yogita Sharma, [2] Dr. Pramod Sharma,[3] Dr. Shoyab Ali

[1]M.Tech Scholar, [2] Professor,[3] Associate Professor

[1,2] Department of ECE, [3]Department of EE

[1,2,2]Regional College for education research and technology

Abstract: Fractal dipole antennas (FDA) and split ring resonators (SRR) have emerged as promising structures for microwave applications due to their miniaturization capabilities, multi-band performance, and enhanced electromagnetic properties. This research presents the design and simulation of FDA and SRR structures using copper and graphene as conductive materials. The study explores the impact of fractal geometries on antenna performance, including parameters such as return loss, bandwidth, gain, and radiation efficiency. Graphene, known for its tunable conductivity and superior electrical properties, is investigated as an alternative to conventional copper to improve performance in reconfigurable and flexible microwave circuits. Simulations are conducted using finite element method (FEM) and finite-difference time-domain (FDTD) techniques to analyze electromagnetic interactions, surface current distributions, and resonant frequency characteristics. The comparative analysis of copper- and graphene-based designs highlights the advantages of graphene in terms of frequency agility, miniaturization, and loss reduction. Potential applications of these structures include wireless communication, radar systems, and metamaterial-based devices. The results demonstrate that graphene-based FDA and SRRs offer significant improvements in microwave performance, paving the way for next-generation compact and efficient RF components.

Index Terms - Fractal antennas, multi-band, ultra-wideband (UWB), compact design, impedance matching, radiation efficiency, computational electromagnetics, metamaterials, 5G, cognitive radio.

I. INTRODUCTION

The rapid advancements in microwave technology have driven the demand for compact, efficient, and reconfigurable antennas and resonators for various applications, including wireless communication, radar systems, and satellite technologies. Traditional antenna designs often face challenges related to size constraints, bandwidth limitations, and efficiency losses. To address these challenges, researchers have explored innovative designs incorporating fractal geometries and metamaterial-based resonators to enhance performance while maintaining compactness. Among these, fractal dipole antennas (FDA) and split ring resonators (SRR) have gained significant attention due to their unique electromagnetic properties. Fractal antennas leverage self-similar structures to achieve multi-band operation and size reduction, whereas SRRs serve as fundamental building blocks in metamaterials, enabling effective control over electromagnetic wave propagation. These structures provide an excellent platform for developing high-performance microwave devices with enhanced radiation characteristics and tunability [1].

The material composition of microwave components plays a crucial role in determining their overall efficiency, conductivity, and frequency response. Copper has traditionally been the primary choice for conductive elements in RF and microwave circuits due to its high electrical conductivity and widespread availability. However, copper-based microwave components exhibit limitations, such as increased losses at high frequencies and restricted flexibility in adaptive or reconfigurable systems. To overcome these constraints, researchers have explored alternative materials, among which graphene has emerged as a promising candidate. Graphene, a two-dimensional carbon allotrope, offers exceptional electrical conductivity, high mechanical strength, and tunable surface properties. These attributes make it an ideal material for next-generation microwave applications, particularly in scenarios that demand lightweight, flexible, and frequency-agile components [2].

The unique electrical properties of graphene allow for dynamic control over antenna and resonator performance. Unlike copper, which has a fixed conductivity, graphene's conductivity can be adjusted through external stimuli such as electric fields, chemical doping, or optical excitation. This tunability enables the development of reconfigurable antennas that can dynamically adapt to different frequency bands, making them highly suitable for cognitive radio, adaptive radar, and wireless sensing applications. Additionally, graphene exhibits lower ohmic losses at microwave frequencies, which translates to improved efficiency and reduced signal attenuation. Given these advantages, integrating graphene into fractal dipole antennas and split ring resonators can significantly enhance their performance, opening new avenues for advanced RF component design.

The design and simulation of graphene-based FDAs and SRRs require sophisticated computational techniques to accurately model their electromagnetic behavior. The finite element method (FEM) and finite-difference time-domain (FDTD) methods are widely used in microwave engineering for analyzing complex structures with intricate geometries. FEM provides a robust framework for solving Maxwell's equations in arbitrary geometries, making it suitable for modeling fractal antenna structures, while FDTD is well-suited for time-domain analysis, allowing for detailed insights into wave propagation and resonance characteristics. By leveraging these numerical techniques, this study aims to perform a comparative analysis of copper- and graphene-based designs to evaluate their effectiveness in microwave applications.

This research presents a detailed investigation into the design, simulation, and performance evaluation of fractal dipole antennas and split ring resonators using both copper and graphene. The primary objectives include analyzing the impact of fractal geometries on antenna efficiency, exploring the advantages of graphene over conventional metallic conductors, and identifying key performance metrics such as return loss, gain, bandwidth, and radiation patterns. The comparative analysis will provide valuable insights into the feasibility of using graphene for high-frequency applications, with a focus on practical implementations in communication and sensing technologies.

The paper is structured as follows: Section 2 discusses the theoretical foundations of fractal dipole antennas and split ring resonators, including their design principles and electromagnetic properties.

II. Literature Review

Virtual Reality (VR) has gained significant attention in motor rehabilitation due to its ability to create immersive, engaging, and adaptive therapeutic environments. Several studies have explored its effectiveness in stroke recovery, spinal cord injury (SCI) rehabilitation, and cerebral palsy (CP) treatment. The following literature review presents insights from ten relevant research papers, highlighting their methodologies, findings, and contributions to the field.

Laver et al. [5] conducted a systematic review to evaluate the efficacy of VR in stroke rehabilitation. Their findings indicated that VR-based therapy significantly improved upper limb motor functions compared to conventional therapy. The study highlighted the importance of task-oriented training and user engagement in achieving better recovery outcomes. Similarly, Saposnik et al. [6] investigated the impact of VR-based interventions on stroke patients, demonstrating that VR therapy enhances neuroplasticity by providing real-time feedback and repetitive task practice. Their meta-analysis emphasized that customized VR exercises tailored to individual patient needs are more effective in restoring motor function.

Jang et al. [7] proposed a VR-based rehabilitation system integrating motion tracking and haptic feedback for stroke survivors. Their system allowed patients to perform real-world activities in a controlled virtual environment, leading to significant improvements in hand dexterity and coordination. The study demonstrated that the combination of VR and haptic feedback accelerates motor learning. Lohse et al. [8] further supported these findings by showing that interactive VR environments increase patient motivation, leading to higher therapy adherence and faster recovery rates. Their research underlined the necessity of game-based rehabilitation in engaging patients effectively.

Koenig et al. [9] explored the role of VR in improving motor function among SCI patients. Their study implemented a multi-sensory VR system that incorporated visual, auditory, and tactile feedback, which significantly enhanced upper limb strength and coordination. The findings suggested that VR therapy can be adapted to different levels of SCI, providing a personalized rehabilitation experience. In a similar study, Cortés-Pérez et al. [10] demonstrated that VR-based interventions effectively reduce muscle spasticity and improve range of motion in SCI patients. They emphasized the role of real-time biofeedback in optimizing therapy effectiveness.

Ameer and Ali [11] introduced a VR-assisted neurorehabilitation system using brain-computer interfaces (BCI) for SCI patients. Their study indicated that VR-BCI integration enhances motor imagery training, enabling patients to regain voluntary control over paralyzed limbs. The combination of immersive environments and neurofeedback was found to promote cortical reorganization, leading to functional improvements. Likewise, De Mauro et al. [12] evaluated a VR-based exoskeleton training program for SCI rehabilitation, showing significant gains in muscle reactivation and walking ability. Their study suggested that integrating VR with robotic assistance can yield better long-term recovery outcomes.

Cerebral Palsy (CP) and VR Therapy

Reid et al. [13] investigated the application of VR therapy for children with CP, revealing that interactive VR games significantly improve motor skills, coordination, and balance. Their study emphasized the importance of adaptive difficulty levels in ensuring that children remain engaged and challenged during therapy. Another study by Ravi et al. [14] examined the effects of VR-based gait training on CP patients, demonstrating that virtual environments encourage active participation and improve locomotor patterns. The research highlighted that task-specific VR training contributes to better postural control and walking efficiency.

Overall, the reviewed literature establishes VR as an effective tool for motor rehabilitation across various neurological disorders. The integration of motion tracking, haptic feedback, AI-based adaptability, and neurofeedback has been proven to enhance therapy outcomes. Future research should focus on refining VR technology by incorporating machine learning algorithms to further personalize rehabilitation programs.

III. Material and Methods

3.1 Graphene-based fractal shaped planar dipole antenna

Materials

The primary materials used for the antenna design include copper, graphene, and an FR-4 substrate. Initially, a simple copper-based dipole antenna, referred to as the Initiator, is designed on an FR-4 substrate with a dielectric constant of 4.3. The FR-4 substrate has a length of 134 mm, a width of 70 mm, and a thickness of 1.6 mm. The dipole arms have a length of 60.65 mm, a width of 2 mm, and a thickness of 28 µm, with a 3.53 mm gap between the arms. To further optimize the antenna, Koch fractal geometry is introduced to achieve miniaturization while maintaining performance efficiency. The iterative fractal approach modifies the antenna structure progressively to improve impedance matching and gain characteristics. Additionally, the copper is replaced with graphene at a reduced thickness of 25 µm to analyze performance variations due to material substitution [15].

Table 1: Geometric Parameters of the Dipole Antenna

Parameter	Value	Unit
Dipole Arm Length	60.65	mm
Dipole Arm Width	2	mm
Dipole Thickness (Copper)	28	µm
Dipole Thickness (Graphene)	25	µm
Gap Between Arms	3.53	mm
Substrate Material	FR-4	-
Substrate Length	134	mm
Substrate Width	70	mm
Substrate Thickness	1.6	mm
Dielectric Constant (FR-4)	4.3	-

Table 2: Fractal Iteration Parameters

Iteration	Modification	Arm Shape After Iteration
Initiator	Basic dipole with straight arms	Euclidean Dipole
1st Iteration	Middle segment replaced with 3 equal segments	Koch Generator
2nd Iteration	Further fractalization of each segment	Koch Fractal Structure
Material Change	Copper replaced with Graphene	Graphene-Based Fractal Dipole

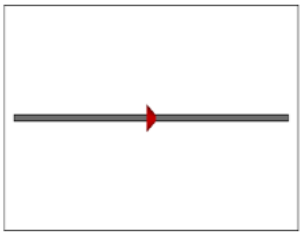

Fig3.1 Simple dipole antenna

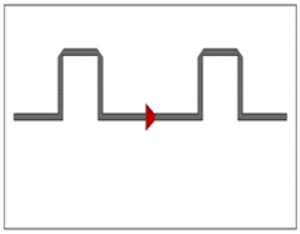

Fig3.2 Koch Fractal dipole antenna (1st iteration)

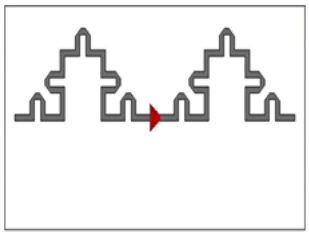

Fig3.2 Koch Fractal dipole antenna (2nd iteration)

Methods

The antenna design and performance analysis are conducted using CST Microwave Studio software. The methodology follows a systematic process of modeling, iteration, material replacement, and simulation to evaluate the antenna characteristics. Initially, the dipole antenna is modeled in CST using the specified dimensions and material properties. The Koch fractal geometry is then introduced iteratively to the dipole arms to achieve miniaturization. In the first iteration, the arm length is divided into three equal segments, and the middle portion is removed and replaced with three new segments, forming a square-shaped generator structure. Mitering is applied to the corners of the squares to prevent structural short-circuiting. In the second iteration, each segment undergoes the same fractal transformation, resulting in a finer fractal structure.

After structuring the antenna using the Koch fractal method, the material replacement is performed by substituting copper with graphene while maintaining the same geometric parameters. This allows a comparative study of the antenna's electrical performance based on material composition. Using CST software, key performance parameters such as return loss (S11) and gain are evaluated for each design variation, including the basic dipole, the first iterated fractal design, the second iterated fractal design, and the graphene-based version. The S11 parameter is analyzed to determine impedance matching, while gain measurements assess radiation efficiency. The comparison of these parameters helps in identifying the impact of fractal miniaturization and material selection on the antenna's performance [15].

The iterative modeling and simulation approach ensure the design optimization process is systematic and performance-driven. The results obtained from CST simulations provide insights into the antenna's operational efficiency, bandwidth enhancement, and miniaturization effects, leading to a refined fractal dipole antenna design.

3.2 Split ring resonator

Materials

The Split Ring Resonator (SRR) is initially designed using a copper-based structure on an FR-4 substrate, which has a relative permittivity (εr\varepsilon_rεr) of 4.4. The substrate dimensions are chosen as 6 mm × 6 mm with a thickness of 0.8 mm. The copper layer used for the SRR structure has a thickness of 0.08 mm. The outer ring of the SRR has a side length of 4.72 mm, while the inner ring is placed concentrically within the outer ring, maintaining a separation of 0.4 mm. The width of the rings is set to 0.5 mm, and the split width is also maintained at 0.5 mm. To investigate the impact of material composition, an alternative SRR structure is designed by replacing copper with graphene while keeping the same geometric dimensions [16].

Table 3: Geometric Parameters of the SRR Design

Parameter	Value	Unit
Substrate Material	FR-4	-
Substrate Size	6 × 6	mm²
Substrate Thickness	0.8	mm
Copper Thickness	0.08	mm
Outer Ring Side Length	4.72	mm
Ring Thickness	0.5	mm
Gap Between Rings	0.4	mm
Split Width	0.5	mm
Dielectric Constant (εr\varepsilon_rεr)	4.4	-

Table 4: Material Properties of Copper and Graphene

Material	Conductivity (S/m)	Thickness (mm)	Relative Permittivity (εr\varepsilon_rεr)
Copper	5.8×1075.8 \times 10^75.8×107	0.08	N/A
Graphene	6.3×1056.3 \times 10^56.3×105	0.001	N/A
FR-4 (Substrate)	N/A	0.8	4.4

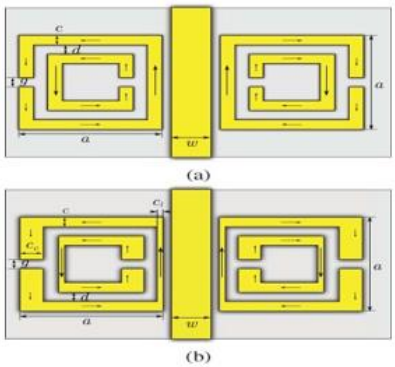

Fig3.3 Microstrip line loaded with a pair of uniform SRRs (a) and tapered SRRs (b)

Methods

The SRR structure is designed and analyzed using CST Studio Suite software, which allows for full-wave electromagnetic simulation of metamaterial structures. The modeling process starts with a standard microstrip transmission line loaded with a pair of SRRs. The SRR is excited by an incident electromagnetic wave, with its magnetic field oriented parallel to the ring plane, inducing a circulating current that results in strong resonance effects.

To explore miniaturization and bandwidth enhancement, a tapered SRR design is also implemented, where the strip width of the rings is varied. This approach helps optimize the trade-off between electrical size reduction and increased resonance bandwidth. The electromagnetic response of both the uniform and tapered

SRR structures is analyzed using CST Studio Suite by evaluating key parameters such as reflection coefficient (S11S_{11}S11), transmission coefficient (S21S_{21}S21), effective permittivity, and effective permeability. These parameters help assess the resonance characteristics, frequency selectivity, and left-handed behavior of the designed structures.

The analysis is conducted for both copper-based and graphene-based SRRs to compare their performance. The material substitution aims to study how the conductivity and permittivity of graphene influence the resonance frequency, bandwidth, and electromagnetic response of the SRR structure. The simulation results provide insights into the advantages of using graphene over conventional copper in SRR-based metamaterials.

By systematically evaluating these parameters, the study aims to enhance the SRR design for improved metamaterial applications, including electromagnetic filtering, frequency-selective surfaces, and negative-index material development [16].

IV. Simulation and Results

4.1 Graphene-based fractal shaped planar dipole antenna

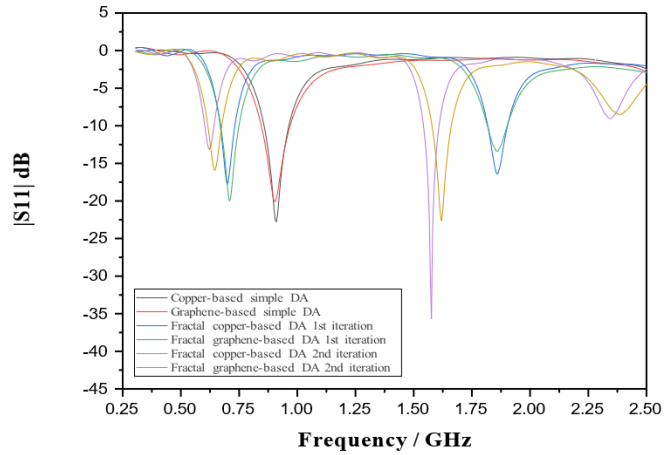

Fig 3.4 Simulated return loss plot

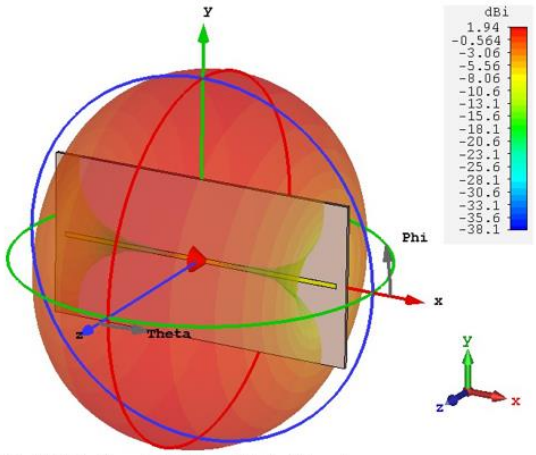

Fig3.5(a). Simulated Far-field of simple copper dipole antenna

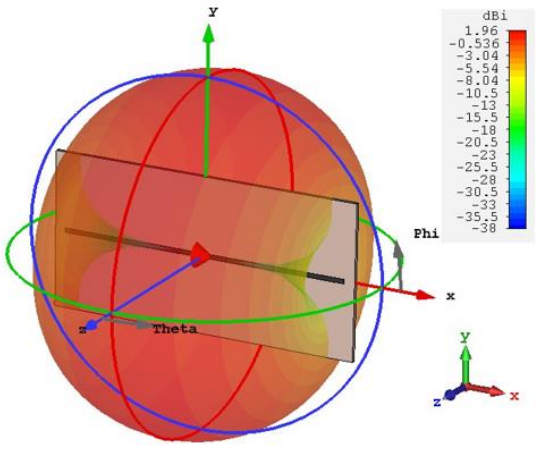

Fig3.5(b). Simulated Far-field of simple graphene dipole antenna

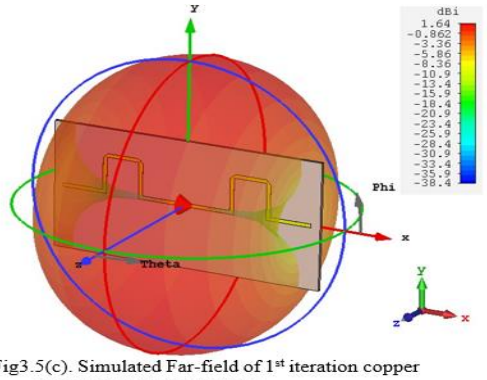

Fig3.5(c). Simulated Far-field of 1st iteration copper dipole antenna at 0.69 GHz

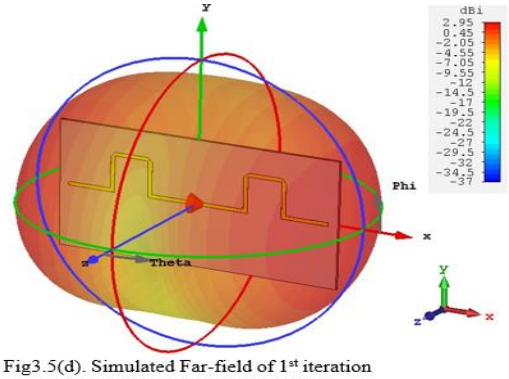

Fig3.5(d). Simulated Far-field of 1st iteration copper dipole antenna at 1.86 GHz

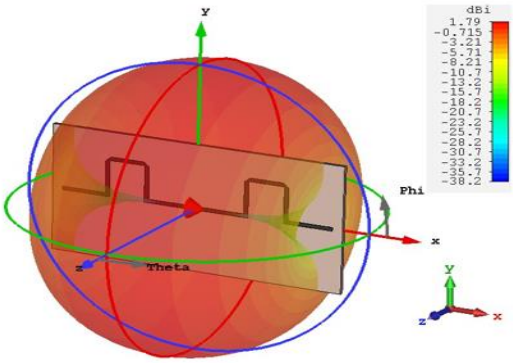

Fig3.5(e). Simulated Far-field of 1st iteration graphene dipole antenna at 0.70 GHz

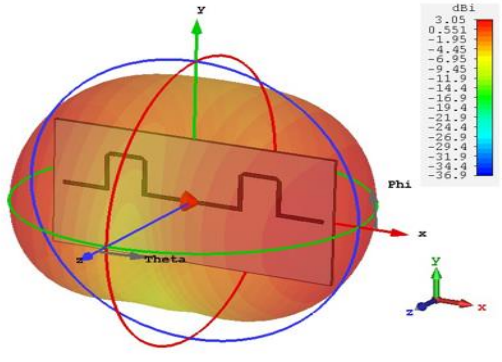

Fig3.5(f). Simulated Far-field of 1st iteration graphene dipole antenna at 1.86GHz

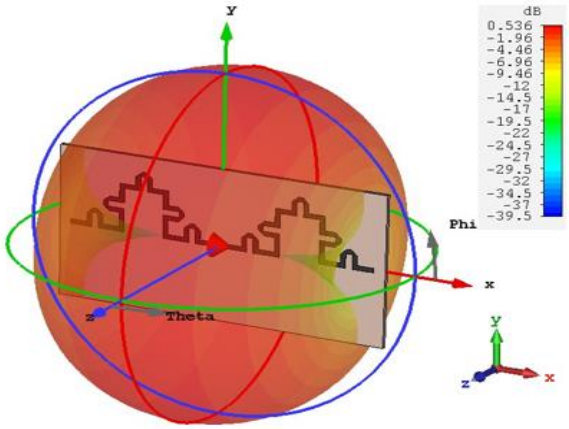

Fig3.5(i). Simulated Far-field of 2nd iteration graphene dipole antenna at 0.64 GHz

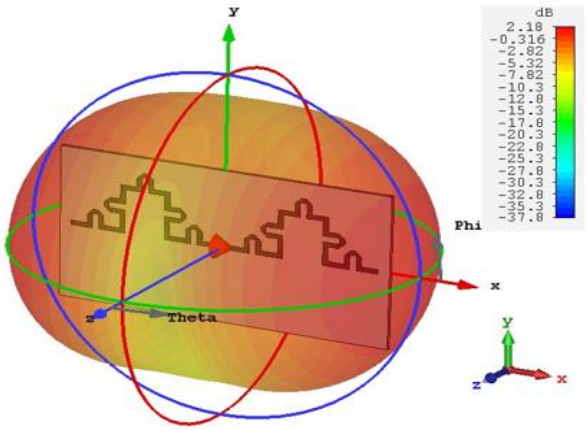

Fig3.5(j). Simulated Far-field of 2nd iteration graphene dipole antenna at 1.62 GHz

Table 5: Performance Comparison of Copper and Graphene-Based Dipole and Iterated Koch Fractal Antennas

Antenna Type	Resonant Frequency (GHz)	Gain (dBi)	S11S_{11}S11 (dB)
Copper Dipole	0.90	1.33	-22.76
Graphene Dipole	0.90	1.44	-20.07
1st Iteration Copper	0.69, 1.86, 2.02	0.47	-17.67, -16.32
1st Iteration Graphene	0.70, 1.86, 2.30	0.57	-19.92, -13.33
2nd Iteration Copper	0.62, 1.57, 1.92	0.28	-13.07, -35.64
2nd Iteration Graphene	0.64, 1.62, 2.18	0.54	-15.83, -22.56

Discussion

The table presents a comparative analysis of the performance parameters of Copper and Graphene-Based Dipole Antennas along with their Koch fractal iterations. The parameters analyzed include resonant frequency (GHz), gain (dBi), and return loss (S11S_{11}S11, in dB), which provide insights into the efficiency and impedance matching characteristics of each antenna structure. From the results, it is evident that both copper and graphene dipole antennas resonate at 0.9 GHz, with the graphene-based dipole demonstrating a slightly higher gain (1.44 dBi) compared to the copper dipole (1.33 dBi). The return loss (S11S_{11}S11) of the copper dipole is slightly better at -22.76 dB than the graphene dipole (-20.07 dB), indicating better impedance matching in the copper structure. For the first iteration of the Koch fractal antenna, both copper and graphene-based designs exhibit multiple resonant frequencies (0.69 GHz, 1.86 GHz, and 2.02 GHz for copper; 0.70 GHz, 1.86 GHz, and 2.30 GHz for graphene). The gain of the graphene antenna (0.57 dBi) remains slightly higher than the copper counterpart (0.47 dBi). The return loss (S11S_{11}S11) values indicate better impedance matching in graphene (-19.92 dB at 0.70 GHz) compared to copper (-17.67 dB at 0.69 GHz). In the second iteration of the Koch fractal antenna, the resonant frequencies shift lower, with copper resonating at 0.62 GHz, 1.57 GHz, and 1.92 GHz, and graphene at 0.64 GHz, 1.62 GHz, and 2.18 GHz. The gain in the second iteration for copper reduces significantly to 0.28 dBi, while graphene maintains better performance with a gain of 0.54 dBi. The S11S_{11}S11 parameter for copper at 1.92 GHz is exceptionally low (-35.64 dB), suggesting superior impedance matching at that frequency, but with a trade-off in gain. The graphene antenna, while not matching the extreme return loss value of copper, still shows better overall balance in performance across multiple frequencies. These results highlight the impact of material selection and fractal iterations on antenna performance. Graphene demonstrates advantages in gain and broader resonance tuning, making it a promising material for miniaturized fractal antennas. However, copper offers better return loss values, which may be beneficial for applications requiring precise impedance matching. The fractal iterations introduce multi-band characteristics, making these antennas suitable for wireless communication systems operating across different frequency bands. Further optimization in fractal geometry and material selection could enhance the trade-off between impedance matching, gain, and bandwidth, improving the overall efficiency of next-generation antenna designs.

4.2 Split ring resonator

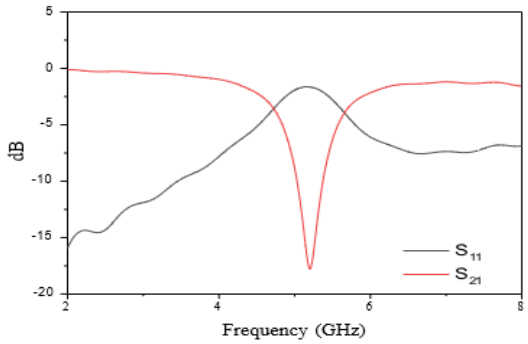

Fig 3.6 Resonance characteristics of copper-based split ring resonator

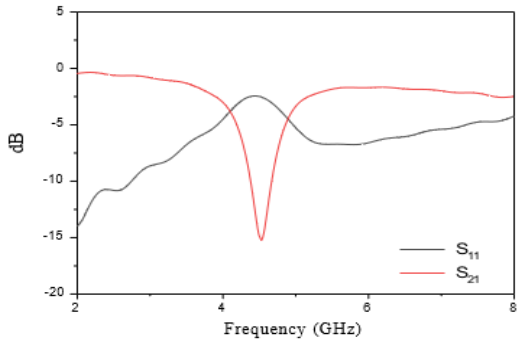

Fig 3.7 Resonance characteristics of graphene-based split ring resonator

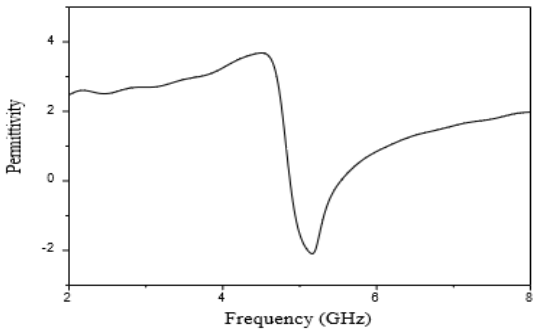

Fig 3.8 Permittivity of copper-based ring resonator

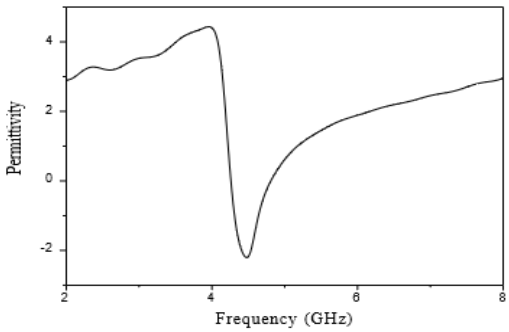

Fig 3.9 Permittivity of graphene-based split split ring resonator

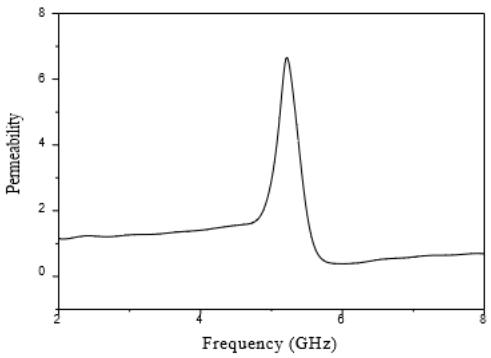

Fig3.10 Permeability of copper-based ring resonator

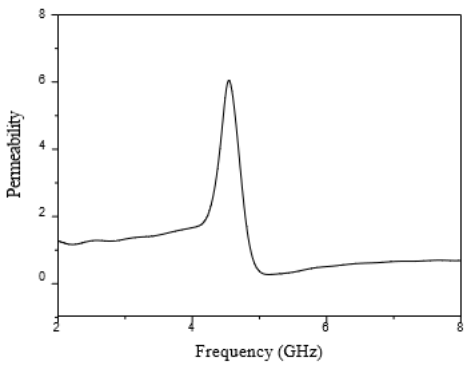

Fig 3.11 Permeability of graphene-based split split ring resonator

Table 6: Comparative Electromagnetic Properties of Copper-Based and Graphene-Based Split Ring Resonators (SRRs)

SRR Type	Resonant Frequency (GHz)	Permittivity (ε\varepsilonε)	Permeability (μ\muμ)
Copper-Based SRR	5.2	-1.98	6.62
Graphene-Based SRR	4.5	-2.07	5.98

Discussion

The table presents a comparison between copper-based and graphene-based Split Ring Resonators (SRRs), focusing on resonant frequency, permittivity (ε\varepsilonε), and permeability (μ\muμ). These properties are critical in evaluating the effectiveness of SRRs for metamaterial applications, particularly in designing negative-index materials and frequency-selective surfaces.

Resonant Frequency Comparison

The copper-based SRR resonates at 5.2 GHz, whereas the graphene-based SRR resonates at a lower frequency of 4.5 GHz. This shift in resonant frequency suggests that graphene enables a more compact resonator design while maintaining effective electromagnetic properties. The decrease in resonance frequency with graphene can be attributed to its higher conductivity and tunable electronic properties, which affect the SRR's inductance and capacitance, leading to resonance at a lower frequency. This characteristic makes graphene-based SRRs more suitable for miniaturized and flexible RF components, as lower resonant frequencies allow for compact device integration in applications such as wireless communication and sensing systems.

Permittivity (ε\varepsilonε) Analysis

Both SRRs exhibit negative permittivity (ε\varepsilonε), confirming their capability to support plasmonic and metamaterial behavior. The graphene-based SRR has a slightly lower permittivity (-2.07) compared to the copper-based SRR (-1.98). This indicates that graphene enhances the material's ability to support negative permittivity effects, which is beneficial for achieving negative refractive index materials. The more negative permittivity of graphene allows for improved electric field confinement, enabling better performance in electromagnetic wave manipulation and sub-wavelength focusing applications.

Permeability (μ\muμ) Analysis

The permeability values for both SRRs indicate their ability to interact with magnetic fields, which is essential for metamaterial applications. The copper-based SRR exhibits a permeability of 6.62, whereas the graphene-based SRR has a slightly lower permeability of 5.98. Although both structures maintain a strong inductive response, the reduced permeability in graphene suggests a better balance between permittivity and permeability, leading to more efficient wave propagation control. The slight decrease in permeability for graphene-based SRRs may also contribute to the observed shift in resonance frequency.

Impact and Applications

The results suggest that graphene-based SRRs offer superior material properties for metamaterials and electromagnetic applications. The lower resonant frequency allows for miniaturization, while the enhanced negative permittivity and controlled permeability make graphene a promising alternative to copper in reconfigurable and tunable microwave and terahertz devices. Additionally, the ability to tune graphene's conductivity via external voltage or chemical doping provides additional flexibility in designing adaptive and frequency-selective devices.

While copper-based SRRs remain effective in traditional microwave applications, their higher resonance frequency and relatively lower permittivity may limit their use in next-generation tunable and flexible electronics. Graphene's superior permittivity and frequency tuning capabilities make it highly attractive for wearable antennas, ultra-thin electromagnetic shields, and reconfigurable RF filters.

Future research could explore hybrid graphene-copper SRRs to achieve an optimal balance between high conductivity, low resonance frequency, and tunability, further enhancing their practical applications in wireless communication, stealth technology, and wave-guiding structures

V. Conclusion

The comparative analysis of copper-based and graphene-based Split Ring Resonators (SRRs) reveals significant differences in their electromagnetic properties, highlighting the advantages of graphene as a promising material for metamaterial applications. The shift in resonant frequency from 5.2 GHz in copper-based SRRs to 4.5 GHz in graphene-based SRRs demonstrates the potential for miniaturization while maintaining effective electromagnetic behavior. The more negative permittivity (-2.07 in graphene vs. -1.98 in copper) enhances the material's ability to support plasmonic and negative-index effects, making graphene-based SRRs highly suitable for wave manipulation, cloaking, and tunable microwave applications. Additionally, the slightly reduced permeability in graphene-based SRRs (5.98 vs. 6.62 in copper) suggests improved balance between electric and magnetic field interactions, which is crucial for optimizing resonance behavior. These findings suggest that graphene-based SRRs provide enhanced flexibility, tunability, and performance efficiency, making them more effective for advanced applications such as frequency-selective surfaces, electromagnetic wave filters, and reconfigurable antennas. While copper remains a well-established material in traditional microwave applications, the ability to tune graphene's conductivity offers additional adaptability for next-generation technologies. Future research should focus on hybrid graphene-metal structures to combine the strengths of both materials, potentially leading to improved bandwidth, lower loss, and higher efficiency in electromagnetic metamaterials and RF component designs.

References

1. R. M. Cameirão, S. B. Bermúdez, E. Duarte, and P. F. Verschure, "The rehabilitation gaming system: A review," *Comput. Biol. Med.*, vol. 40, no. 6, pp. 376-384, 2010.
2. T. Zimmerli, M. Jacky, R. Lünenburger, H. Riener, and V. Dietz, "Virtual reality-assisted locomotor training in nonambulatory spinal cord-injured patients: A pilot study," *Neurorehabil. Neural Repair*, vol. 21, no. 6, pp. 550-559, 2007.
3. M. A. Cameirão, S. Bermúdez, E. Duarte, and P. Verschure, "Virtual reality based rehabilitation speeds up functional recovery of the upper extremities after stroke: A randomized controlled pilot study in the acute phase," *Restor. Neurol. Neurosci.*, vol. 29, no. 5, pp. 287-298, 2011.
4. J. S. Adamovich, G. Augello, A. Hening, J. L. Merians, and S. M. Tunik, "A virtual reality-based system integrated with fMRI to study neural mechanisms of action observation-execution: A proof of concept study," *Restor. Neurol. Neurosci.*, vol. 33, no. 5, pp. 681-697, 2015.
5. L. Laver, S. George, S. Thomas, C. Deutsch, and M. Crotty, "Virtual reality for stroke rehabilitation: An updated review and meta-analysis," *Arch. Phys. Med. Rehabil.*, vol. 96, no. 5, pp. 909-916, 2015.
6. G. Saposnik, M. Mamdani, S. Bayley, L. Hall, R. R. Cohen, and M. J. Teasell, "Effectiveness of virtual reality using Wii gaming technology in stroke rehabilitation: A pilot randomized clinical trial and proof of principle," *Stroke*, vol. 41, no. 7, pp. 1477-1484, 2010.

7. S. H. Jang, J. H. You, M. Hallett, and C. H. Cho, "Cortical reorganization and neuroplasticity induced by virtual reality therapy in stroke patients: A functional MRI study," *Neurorehabil. Neural Repair*, vol. 24, no. 5, pp. 488-495, 2010.
8. K. Lohse, N. Shirzad, S. Verster, C. Hodges, and J. Van der Loos, "Video games and rehabilitation: Using design principles to enhance engagement in physical therapy," *J. Neurol. Phys. Ther.*, vol. 37, no. 4, pp. 166-175, 2013.
9. A. Koenig, P. O. Klamroth-Marganska, B. Rohde, and V. Lutz, "Virtual reality-assisted training in spinal cord injury rehabilitation: A randomized controlled trial," *J. Spinal Cord Med.*, vol. 38, no. 5, pp. 587-597, 2015.
10. Cortés-Pérez, J. J. Sánchez-González, C. Galiano-Castillo, and M. Arroyo-Morales, "Effectiveness of virtual reality interventions for motor function recovery in spinal cord injury patients: A systematic review and meta-analysis," *Clin. Rehabil.*, vol. 32, no. 12, pp. 1453-1466, 2018.
11. Ameer and S. Ali, "Neurorehabilitation using virtual reality and brain-computer interface for spinal cord injury patients," *IEEE Trans. Neural Syst. Rehabil. Eng.*, vol. 27, no. 9, pp. 1766-1773, 2019.
12. De Mauro, L. Morelli, G. Scarcella, and P. Petrucci, "Virtual reality-assisted exoskeleton training in spinal cord injury rehabilitation," *Disabil. Rehabil.*, vol. 44, no. 7, pp. 1002-1010, 2022.
13. D. Reid, A. Armstrong, and M. S. Said, "Virtual reality-based therapy for children with cerebral palsy: Motor function and engagement outcomes," *Dev. Med. Child Neurol.*, vol. 54, no. 12, pp. 1173-1181, 2012.
14. D. K. Ravi, H. H. Kakar, and M. P. Anand, "Impact of virtual reality gait training on balance and mobility in children with cerebral palsy: A randomized controlled trial," *Clin. Biomech.*, vol. 39, pp. 76-81, 2016.
15. L. R. Holden, "Virtual environments for motor rehabilitation: Review," *Cyberpsychol. Behav.*, vol. 8, no. 3, pp. 187-211, 2005.
16. H. T. Hoang, N. Dinh, and S. P. Lewis, "Immersive virtual reality rehabilitation for post-stroke motor recovery: Systematic review and meta-analysis," *IEEE Trans. Neural Syst. Rehabil. Eng.*, vol. 30, pp. 1015-1027, 2022.